cells (Figures 4J–4L′). The transition and Lgr5 expression is blocked by the addition of porcupine inhibitor to ENR-supplemented cultures (Figures 4I, 4I′, and 4N) and by the addition of the tankyrase inhibitor IWR-1 to cells cultured in the presence of ENR and Wnt (Figures 4M, 4M′, and 4N). Importantly, these inhibitors do not preclude the formation of FEnS. The maturation is reflected at the RNA level, where Wnt induces a robust increase in the Paneth cell marker Lysozyme. However, it is also clear that FEnS in early cultures express endogenous *Wnt3a*, which drives both *Axin2* and *Lgr5* expression within the fetal population of cells (Figure 4O). In line with the elevated expression of *Axin2* and *Lgr5*, β-catenin can be observed in the nucleus of cells in FEnS as well as in the formed organoids (Figures 4P and 4Q).

In vivo tissue maturation correlates with the emergence of secretory Paneth cells, which has been identified as the major source of epithelial Wnt secretion in the intestinal epithelium (Sato et al., 2011b; Farin et al., 2012). Although mature Lysozyme^{-ve} Paneth cells cannot be observed until postnatal week 2 (Figure sS2E–S2H), these are preceded by immature secretory cells, which can be detected based on *Cryptdin6* expression (Wong et al., 2012). Assessment of tissues from P2 and P15 demonstrates that *Cryptdin6*-expressing cells can be detected as early as P2 (Figures 4R and 4S). This correlates with the appearance of cells that are weakly positive for the stem cell marker *Olfm4* as well as *Wnt3a* within the bottom of the intervillus regions (Figures 4T–4W). This provides an epithelial source of Wnt3a that can drive tissue maturation.

In summary, this demonstrates that exogenous Wnt induces elevated focal Lgr5 upregulation in the fetal state and that maturation proceeds from these Lgr5 expression domains. Expression of *Wnt3a* can be detected in proliferative intervillus regions as the tissue proceeds into its adult state, suggesting that Wnt induction in vivo correlates with tissue maturation.

Regeneration of Adult Colonic Epithelium from mFEnS

To assess the differentiation potential of immature intestinal progenitors and whether they represent a transplantable source, EGFP^{+ve} established mFEnS were injected under the renal capsule of mice (n = 8). In all cases at analysis, EGFP FEnS cells had either not proliferated or were not detectable. To test a more physiologically relevant approach, we transplanted EGFP FEnS into a chemically induced colonic injury model, where the repair process is associated with endogenous activation of Wnt signaling (Figure 5A; Yui et al., 2012; Koch et al., 2011). Within 3 hr after the first transplantation, FEnS-derived cells attached to ulcerated regions in the distal colon and were subsequently maintained long-term (Figures 5B and S5A–S5H). Initially, cells engrafted as a single-layered epithelium on top of the denuded lamina propria (Figures S5I–S5J). Three days following transplantation, grafted regions migrated downward into the underlying mesenchyme. Here they formed epithelial "pockets" with a central lumen and Ki67^{+ve} cells distributed along the length (Figures 5C, S5K, and S5L). One week after the second transplantation, engrafted cells formed epithelial crypt-like structures. These fetal-derived cells, although refractory to maturation in vitro, adapt to the colonic tissues, with subsets of cells differentiating appropriately into Mucin-2^{+ve} and PAS^{+ve} goblet cells and starting to express carbonic anhydrase-II, a specific marker of colonic tissue. None of this was detected in FEnS (Figures 5C, S5L, S5N, and S5P–S5R). Importantly, the grafted material did not express markers normally associated with the small intestine such as Lysozyme and alkaline-phosphatase (Figures S5R–S5T). Fetal-derived colonic crypts persisted at 1.5 months after transplantation, with continued evidence for proper differentiation and proliferation (Figures 5C, S5O, and S5P). Thus, immature enteric progenitors represent a transplantable source of cells with the capacity to differentiate in vivo.

DISCUSSION

In this study, we reveal the existence of a transitory population of progenitors present during the intestinal growth phase in both human and murine tissues. Moreover, a population of cells with similar characteristics can be obtained from pluripotent stem cells. This population is characterized by distinct proliferative and differentiation potential and reduced in vitro growth factor requirements compared to progenitors in the adult intestinal epithelium. Transition of fetal enteric progenitors into an adult state can be induced in vitro via stimulation with high levels of Wnt or alternatively by transplantation in vivo into an injury model. These cells are a valuable asset for understanding tissue maturation and an attractive source of transplantable progenitors for regenerative therapies.

Studies of human organ development are complicated by the availability of material. We provide evidence that mouse and human fetal intestine contain an immature population of epithelial progenitors and that similar immature cells can be obtained from hPSCs. Here the immature progenitors represent a transitory population of cells. Interestingly, many differentiation protocols from PSCs result in cells with a stable immature phenotype (Meyer et al., 2009; Nicholas et al., 2013). Based on our results this is not necessarily a tissue culture artifact but rather a result of the in vitro stabilization of an otherwise transitory state in vivo. It is however clear that it is not straightforward to extrapolate growth factor requirements from mouse to human cells as has been reported for their adult counterparts (Jung et al., 2011; Sato et al., 2009, 2011a).

Intestinal maturation has been proposed to follow a rostral-to-caudal (proximal-to-distal) wave (Spence et al., 2011a). We observe that FEnS form from the proximal region and organoids from the distal region, indicating that maturation in actual fact proceeds in the opposite direction. This is correlated with the expression pattern of markers of the mature secretory lineage and correlates with the observation that Lgr5 expression is associated with progenitors in a transitory competent state. These spatial and temporal observations are in agreement with previous work showing that Lgr5 gene expression is higher in the ileum than in the duodenum at E18.5 (García et al., 2009). It

(R–W) In situ hybridization for *Cryptdin6*, *Olfm4*, and *Wnt3a* in tissue from P2 and P15. Arrows in (S) and (U) indicate regions of Olfm4 and Wnt3a expression, respectively.

The scale bars represent 50 μm (F, J, K–L, P–Q, and V–W) or 100 μm (A, D–E, G–I, M, and R–U). Cells are counterstained with DAPI (blue) in (A), (O), and (P). See also Figure S4 and Movie S1, Movie S2, and Movie S3.

Please cite this article in press as: Fordham et al., Transplantation of Expanded Fetal Intestinal Progenitors Contributes to Colon Regeneration after Injury, Cell Stem Cell (2013), http://dx.doi.org/10.1016/j.stem.2013.09.015

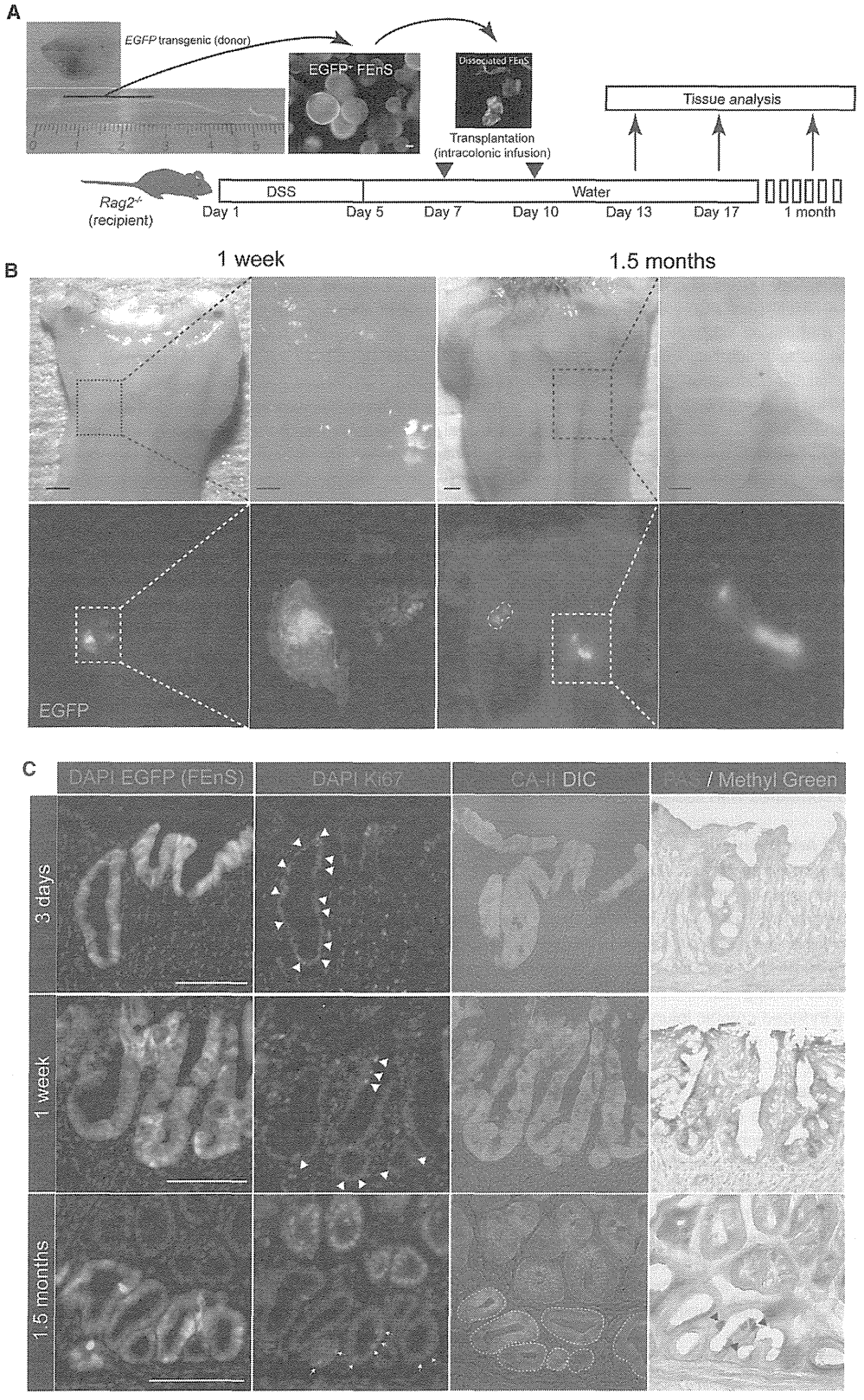

(legend on next page)

does remain a possibility that the culture conditions that maintain adult stem cells in vitro are optimal for the distal intestine at this developmental time point rather than a reflection of tissue maturation.

The spatial differences in expression of the Wnt target genes *Lgr5* and *Axin2* (Barker et al., 2007; Lustig et al., 2002) prompted the investigation of Wnt signaling in the developmental transition. The differing requirements between the mature and immature states imply that Wnt signaling has a context-dependent role in development and tissue homeostasis or alternatively that ligands are dynamically regulated. There are several potential Wnt ligands in the intestine, where Wnt3a has been shown to play an autonomous role in epithelial stem cell maintenance (Sato et al., 2011b; Farin et al., 2012). In line with this, we observe that the expression of Wnt3a is correlated with the appearance of adult stem cell markers as well as adult stem cell behavior in the developing epithelium. Interestingly, this pattern of expression coincides with the phenotype of the knockout of the major β-catenin effector, Tcf4, which die shortly after birth with intestinal hypoplasia (Korinek et al., 1998).

In vitro Wnt stimulation and spontaneous maturation can be blocked by Wnt inhibition. Here, Wnt causes a prominent focal upregulation of Lgr5 expression in the developing structures. This is associated with the transition from a thin epithelium to domains with columnar morphology reminiscent of the cellular architecture in the small intestine. After the emergence of Paneth cells, these structures become independent of exogenous Wnt similar to adult intestinal stem cells. We hypothesize that Lgr5 in this context facilitates the transition by enhancing focal Wnt stimulation via the Wnt agonist R-spondin1 (de Lau et al., 2011). This will also explain why established FEnS are resilient to Wnt stimulation in vitro—they express significantly reduced levels of Lgr5. Although Wnt signaling mediates the transitioning of murine FEnS, it might be more complicated for hFEnS, where a low level of Wnt stimulation is required for their normal maintenance.

The gold standard for testing the true differentiation potential of progenitor cells is in vivo transplantation (Lin et al., 2013). We have previously demonstrated that adult colonic organoids can engraft into an injury model (Yui et al., 2012). An initial concern was that due to the striking morphological and growth similarities between FEnS and APC null adult organoids (Sato et al., 2011b), transplantation of FEnS in vivo would lead to tumor formation. However, FEnS cells were shown to attach to denuded regions of colonic epithelium and subsequently be incorporated into the colonic epithelium. Furthermore, since FEnS were unable to survive under the kidney capsule, this suggests that orthotopic transplantation is a more useful readout of in vivo potential. Our transplantation experiments unequivocally demonstrate that established FEnS can mature in vivo and contribute to regeneration of damaged gut epithelium in adult hosts. Moreover, it is striking that these fetal derivatives from the small intestine rapidly respond to the new microenvironment and differentiate appropriately to the regional requirements. This might reflect their immature behavior although we cannot exclude the possibility that adult organoids will behave similarly.

In summary, we have identified a population of expandable fetal enteric progenitors from mouse and human that can be used as a transplantable source. This work has important implications for understanding the mechanisms underlying intestinal maturation and demonstrates that immature intestinal progenitors, including fetal-like material derived from human pluripotent stem cells, have the potential to be used in colonic regenerative medicine. It will be interesting to see if similar populations of immature progenitors exist in other endodermal organs.

EXPERIMENTAL PROCEDURES

Mice

Rag2$^{-/-}$ mice were from Taconic Farms and Central Laboratories for Experimental Animals. *EGFP* transgenic mice and Lgr5-EGFP-ires-CreERT2 mice are described elsewhere (Barker et al., 2007; Okabe et al., 1997). Experimental animals were obtained by crossing these with C57BL/6 male or female animals. All animal experiments in Cambridge were performed under the terms of a UK Home Office License and transplantation experiments were performed with the approval of the Institutional Animal Care and Use committee of TMDU.

Transplantation

Transplantation was performed as described on days 7 and 10 following initiation of dextran sulfate sodium-induced colonic injury (Yui et al., 2012). Donor FEnS were released from the Matrigel and mechanically dissociated into small sheets of epithelial tissue. Cell fragments from 500–1,000 FEnS were resuspended in 200 μl of Matrigel in PBS (1:20), which was instilled into the colonic lumen using a syringe and a thin flexible catheter. Animals were subsequently sacrificed at indicated time points.

In Vitro Cultures

Organoids

Primary crypts from proximal adult small intestine were cultured as previously described with reduced concentration of murine recombinant R-spondin1 (500 ng/ml, R&D Systems; Sato et al., 2009).

FEnS

Fetal small intestines were opened longitudinally and cut into small pieces prior to dissociation with 2 mM EDTA. Isolated epithelial units were embedded in Matrigel and maintained in conditions identical to those used for adult organoids. In certain experiments Wnt3a and R-spondin1 from conditioned media were collected from HEK293 cell lines expressing recombinant Wnt3a and R-spondin1 (kindly provided by Hans Clevers and Calvin Kuo, respectively). Relative Wnt/R-spondin1 activity was measured using a TOPflash assay with a Dual-Luciferase Reporter Assay System (Millipore).

Human Tissue

First-trimester human fetal material was obtained from the John van Geest Centre for Brain Repair, University of Cambridge, and used with informed consent under an Approved Protocol of Human Tissue Studies. Fetuses were staged by Crown Rump Length. Fetal intestines were processed for in vitro epithelial culture, paraffin sections, or RNA extraction, using procedures

Figure 5. Regeneration of Adult Colonic Epithelium from mFEnS

(A) Experimental protocol: gastrointestinal tract dissected from E16 EGFP transgenic mouse fetus (top left). Proximal small intestine was cultured in vitro as FEnS before mechanical dissociation and intracolonic transplantation into *Rag2*$^{-/-}$ adult recipients with Dextran Sulfate Sodium (DSS)-induced ulcerative colitis.

(B) Recipient colon at 1 week and 1.5 months posttransplantation. Lower panel shows EGFP^{+ve} areas in host colon.

(C) Immunohistological analysis of EGFP^{+ve} fetal-derived engraftments for Ki67 (Ki67^{+ve} cells marked by arrowheads), carbonic anhydrase II, and PAS, 3 days, 1 week, and 1.5 months after transplantation.

The scale bars represent 1 mm (whole colons) and 200 μm (magnified areas) in (B) and 100 μm in (C). See also Figure S5.

identical to those described for murine material, with the addition of PGE2 (2.5 μM, Sigma-Aldrich). Adult human intestinal biopsies were obtained from the Division of Gastroenterology and Hepatology, Department of Medicine, University of Cambridge, and were used with local ethical permission, under informed consent.

Adult primary human organoids were derived from biopsies obtained during routine colonoscopies from the terminal ileum. A single crypt suspension was obtained through chelation of the washed biopsies in cold chelation buffer (distilled water with 5.6 mmol/l Na_2HPO_4, 8.0 mmol/l KH_2PO_4, 96.2 mmol/l NaCl, 1.6 mmol/l KCl, 43.4 mmol/l sucrose, 54.9 mmol/l D-sorbitol, 0.5 mmol/l DL-dithiothreitol) containing 4 mM EDTA for 45 min followed by release of the crypts in fresh chelation buffer by vigorous shaking. Isolated crypts were treated like murine and fetal tissues; however, cultures were additionally supplemented with 1xN2 and 1xB27 (from invitrogen), 2.5 mM *N*-acetylcysteine (Sigma), 40% Wnt3a conditioned medium, 10% R-spondin1 conditioned medium, 10 mM nicotinamide, 10 μM SB202190, and 500 nM A-83-01. Tissue for primary human cultures was obtained at Herlev Hospital with local ethical permission and under informed consent.

Generation, Culture, and Differentiation of hiPSCs

hiPSCs (BBHX8) were derived using retrovirus-mediated reprogramming of human skin fibroblasts (Rashid et al., 2010). hiPSCs were cultured in a chemically defined, feeder-free culture system (Brown et al., 2011). Cells were passaged every 7 days using a mixture of collagenase IV or collagenase and dispase at a ratio of 1:1. hiPSCs were differentiated as outlined in Figure S1 and Table S1 (Hannan et al., 2013). Briefly, iPSCs were differentiated into DE using Activin-A, BMP4, and LY294002 for 3 days. DE cells were subsequently cultured with CHIR99021 for 4 days to generate posterior endoderm. Raised aggregates of posteriorized endoderm were transferred into growth factor-reduced Matrigel. The cell-Matrigel mix was overlaid with Advanced DMEM/F12 supplemented with 2 mM GlutaMax (Invitrogen), 10 mM HEPES, and 100 U/ml Penicillin/100 mg/ml Streptomycin containing B27 supplement, Y-27632 (10 mM), human Noggin (100 ng/ml), human EGF (100 ng/ml), human R-spondin1 (1 mg/ml), and human Wnt3a (100 ng/ml).

Imaging and Histology

Live imaging of 3D cultures was performed using a Nikon Biostation IM system. Structures in Matrigel were observed using phase contrast and DIC microscopy using an Axiovert 200M microscope (Zeiss) equipped with an AxioCam MRc (Zeiss).

Tissue preparation, staining, and image analysis were carried out as described previously using antibodies listed in Table S2 (Wong et al., 2012; Yui et al., 2012). Images of sections were acquired using a DeltaVision system (Applied Precision) or a Zeiss Imager M.2, equipped with AxioCam MRm and MRc cameras.

DIG in situ hybridization was carried out essentially as described before using IMAGE clones (Gregorieff et al., 2005).

RNA Extraction and qRT-PCR

RNA was isolated from intact intestine as described (Wong et al., 2012). Total RNA was isolated from cultured cells using the Invitrogen PureLink RNA micro kit. cDNA was synthesized from 100 ng total RNA using the Invitrogen SuperScript III Reverse transcriptase kit, using random primers. Gene-specific expression assays (Applied Biosystems) or SYBR Green analysis (Invitrogen) with optimized primer pairs was used for qPCR on an Applied Biosystems 7500HT RealTime PCR System (Applied Biosystems). Values were normalized to 18S using the ΔCt method. Z scores were calculated and used to generate heatmaps in R.

Isolation of Cells for Flow Cytometry

Cells were isolated essentially as described (Wong et al., 2012). A single-cell suspension was achieved by subsequent incubation using trypsin. Cell sorting was carried out using a MoFlo (Beckman Coulter). Ten thousand cells were seeded into 25 μl Matrigel. Data analysis was performed in FlowJo.

Statistical Analysis

Statistical significance of quantitative data was determined by applying a two-tailed Student's t test to raw values or to the average values obtained from analysis of independent experiments. A two-tailed Fisher's exact test was used to analyze the significance of the Wnt and inhibitor culture experiment.

SUPPLEMENTAL INFORMATION

Supplemental Information for this article includes five figures, two tables, and two movies and can be found with this article online at http://dx.doi.org/10.1016/j.stem.2013.09.015.

AUTHOR CONTRIBUTIONS

R.P.F., S.Y., and K.B.J. conceived and designed the study, analyzed the data, and wrote the manuscript; R.P.F., S.Y., N.R.F.H., C.S., A.M., P.J.S., and K.B.J performed experimental work; and R.P.F., S.Y., and K.B.J. prepared the figures. O.H.N., L.V., R.A.P., and M.W. gave conceptual advice. T.N. and K.B.J supervised the project.

ACKNOWLEDGMENTS

We thank F. Watt for EGFP transgenic mice, SCI Core Facilities for their support, and R. Barker for facilitating access to human fetal tissue. We thank A. Martinez-Arias, B. Simons, M. Zilbauer, and the Jensen, Pedersen, and Watanabe labs for critical discussions. This work was supported by an MRC PhD Studentship and Centenary Awards (R.P.F.), the Regenerative Medicine Realization Base Network Program from Japan Science and Technology Agency (JST) (T.N. and M.W.), the MEXT/JSPS KAKENHI (Grant Number 22229005 to T.N. and M.W.), a Health and Labor Sciences Research Grant for Research on rare and intractable diseases from the Ministry of Health, Labor and Welfare of Japan (M.W.), Sidney Sussex College (A.M.), The Danish Cancer Society (K.B.J.), a Wellcome Trust Career Development Fellowship (K.B.J.), and a Lundbeck Foundation Fellowship (K.B.J.). L.V. is a founder and shareholder of DefiniGEN.

Received: May 22, 2013
Revised: September 4, 2013
Accepted: September 27, 2013
Published: October 17, 2013

REFERENCES

Barker, N., van Es, J.H., Kuipers, J., Kujala, P., van den Born, M., Cozijnsen, M., Haegebarth, A., Korving, J., Begthel, H., Peters, P.J., and Clevers, H. (2007). Identification of stem cells in small intestine and colon by marker gene Lgr5. Nature *449*, 1003–1007.

Barker, N., van Oudenaarden, A., and Clevers, H. (2012). Identifying the stem cell of the intestinal crypt: strategies and pitfalls. Cell Stem Cell *11*, 452–460.

Brown, S., Teo, A., Pauklin, S., Hannan, N., Cho, C.H.-H., Lim, B., Vardy, L., Dunn, N.R., Trotter, M., Pedersen, R., and Vallier, L. (2011). Activin/Nodal signaling controls divergent transcriptional networks in human embryonic stem cells and in endoderm progenitors. Stem Cells *29*, 1176–1185.

de Lau, W., Barker, N., Low, T.Y., Koo, B.K., Li, V.S., Teunissen, H., Kujala, P., Haegebarth, A., Peters, P.J., van de Wetering, M., et al. (2011). Lgr5 homologues associate with Wnt receptors and mediate R-spondin signalling. Nature *476*, 293–297.

Farin, H.F., Van Es, J.H., and Clevers, H. (2012). Redundant sources of Wnt regulate intestinal stem cells and promote formation of Paneth cells. Gastroenterology *143*, 1518–1529, e1517.

Garcia, M.I., Ghiani, M., Lefort, A., Libert, F., Strollo, S., and Vassart, G. (2009). LGR5 deficiency deregulates Wnt signaling and leads to precocious Paneth cell differentiation in the fetal intestine. Dev. Biol. *331*, 58–67.

Gregorieff, A., Pinto, D., Begthel, H., Destrée, O., Kielman, M., and Clevers, H. (2005). Expression pattern of Wnt signaling components in the adult intestine. Gastroenterology *129*, 626–638.

Hannan, N.R.F., Fordham, R.P., Moignard, V., Jensen, K.B., and Vallier, L. (2013). Generation of Multipotent Foregut Stem Cells from Human Pluripotent Stem Cells. Stem Cell Reports *1*, ■■■–■■■.

Jung, P., Sato, T., Merlos-Suárez, A., Barriga, F.M., Iglesias, M., Rossell, D., Auer, H., Gallardo, M., Blasco, M.A., Sancho, E., et al. (2011). Isolation and in vitro expansion of human colonic stem cells. Nat. Med. *17*, 1225–1227.

Koch, S., Nava, P., Addis, C., Kim, W., Denning, T.L., Li, L., Parkos, C.A., and Nusrat, A. (2011). The Wnt antagonist Dkk1 regulates intestinal epithelial homeostasis and wound repair. Gastroenterology *141*, 259–268, 268.e1–8.

Korinek, V., Barker, N., Moerer, P., van Donselaar, E., Huls, G., Peters, P.J., and Clevers, H. (1998). Depletion of epithelial stem-cell compartments in the small intestine of mice lacking Tcf-4. Nat. Genet. *19*, 379–383.

Lin, H.-T., Otsu, M., and Nakauchi, H. (2013). Stem cell therapy: an exercise in patience and prudence. Philos. Trans. R. Soc. Lond. B Biol. Sci. *368*, 20110334.

Lustig, B., Jerchow, B., Sachs, M., Weiler, S., Pietsch, T., Karsten, U., van de Wetering, M., Clevers, H., Schlag, P.M., Birchmeier, W., and Behrens, J. (2002). Negative feedback loop of Wnt signaling through upregulation of conductin/axin2 in colorectal and liver tumors. Mol. Cell. Biol. *22*, 1184–1193.

Meyer, J.S., Shearer, R.L., Capowski, E.E., Wright, L.S., Wallace, K.A., McMillan, E.L., Zhang, S.-C., and Gamm, D.M. (2009). Modeling early retinal development with human embryonic and induced pluripotent stem cells. Proc. Natl. Acad. Sci. USA *106*, 16698–16703.

Montgomery, R.K., Mulberg, A.E., and Grand, R.J. (1999). Development of the human gastrointestinal tract: twenty years of progress. Gastroenterology *116*, 702–731.

Nicholas, C.R., Chen, J., Tang, Y., Southwell, D.G., Chalmers, N., Vogt, D., Arnold, C.M., Chen, Y.-J.J., Stanley, E.G., Elefanty, A.G., et al. (2013). Functional maturation of hPSC-derived forebrain interneurons requires an extended timeline and mimics human neural development. Cell Stem Cell *12*, 573–586.

Okabe, M., Ikawa, M., Kominami, K., Nakanishi, T., and Nishimune, Y. (1997). 'Green mice' as a source of ubiquitous green cells. FEBS Lett. *407*, 313–319.

Rashid, S.T., Corbineau, S., Hannan, N., Marciniak, S.J., Miranda, E., Alexander, G., Huang-Doran, I., Griffin, J., Ahrlund-Richter, L., Skepper, J., et al. (2010). Modeling inherited metabolic disorders of the liver using human induced pluripotent stem cells. J. Clin. Invest. *120*, 3127–3136.

Sato, T., Vries, R.G., Snippert, H.J., van de Wetering, M., Barker, N., Stange, D.E., van Es, J.H., Abo, A., Kujala, P., Peters, P.J., and Clevers, H. (2009). Single Lgr5 stem cells build crypt-villus structures in vitro without a mesenchymal niche. Nature *459*, 262–265.

Sato, T., Stange, D.E., Ferrante, M., Vries, R.G.J., Van Es, J.H., Van den Brink, S., Van Houdt, W.J., Pronk, A., Van Gorp, J., Siersema, P.D., and Clevers, H. (2011a). Long-term expansion of epithelial organoids from human colon, adenoma, adenocarcinoma, and Barrett's epithelium. Gastroenterology *141*, 1762–1772.

Sato, T., van Es, J.H., Snippert, H.J., Stange, D.E., Vries, R.G., van den Born, M., Barker, N., Shroyer, N.F., van de Wetering, M., and Clevers, H. (2011b). Paneth cells constitute the niche for Lgr5 stem cells in intestinal crypts. Nature *469*, 415–418.

Spence, J.R., Lauf, R., and Shroyer, N.F. (2011a). Vertebrate intestinal endoderm development. Dev. Dyn. *240*, 501–520.

Spence, J.R., Mayhew, C.N., Rankin, S.A., Kuhar, M.F., Vallance, J.E., Tolle, K., Hoskins, E.E., Kalinichenko, V.V., Wells, S.I., Zorn, A.M., et al. (2011b). Directed differentiation of human pluripotent stem cells into intestinal tissue in vitro. Nature *470*, 105–109.

Wong, V.W.Y., Stange, D.E., Page, M.E., Buczacki, S., Wabik, A., Itami, S., van de Wetering, M., Poulsom, R., Wright, N.A., Trotter, M.W.B., et al. (2012). Lrig1 controls intestinal stem-cell homeostasis by negative regulation of ErbB signalling. Nat. Cell Biol. *14*, 401–408.

Yui, S., Nakamura, T., Sato, T., Nemoto, Y., Mizutani, T., Zheng, X., Ichinose, S., Nagaishi, T., Okamoto, R., Tsuchiya, K., et al. (2012). Functional engraftment of colon epithelium expanded in vitro from a single adult Lgr5^{+} stem cell. Nat. Med. *18*, 618–623.

Zorn, A.M., and Wells, J.M. (2009). Vertebrate endoderm development and organ formation. Annu. Rev. Cell Dev. Biol. *25*, 221–251.

T-helper 17 and Interleukin-17–Producing Lymphoid Tissue Inducer-Like Cells Make Different Contributions to Colitis in Mice

YUICHI ONO,* TAKANORI KANAI,* TOMOHISA SUJINO,* YASUHIRO NEMOTO,‡ YASUMASA KANAI,* YOHEI MIKAMI,* ATSUSHI HAYASHI,* ATSUHIRO MATSUMOTO,* HIROMASA TAKAISHI,* HARUHIKO OGATA,§ KATSUYOSHI MATSUOKA,* TADAKAZU HISAMATSU,* MAMORU WATANABE,‡ and TOSHIFUMI HIBI*

*Division of Gastroenterology and Hepatology, Department of Internal Medicine, and §Center for Diagnostic and Therapeutic Endoscopy, Keio University School of Medicine, Tokyo; ‡Department of Gastroenterology and Hepatology, Graduate School, Tokyo Medical and Dental University, Tokyo, Japan

BACKGROUND & AIMS: T helper (Th) 17 cells that express the retinoid-related orphan receptor (ROR) γt contribute to the development of colitis in mice, yet are found in normal and inflamed intestine. We investigated their development and functions in intestines of mice. **METHODS:** We analyzed intestinal Th17 cells in healthy and inflamed intestinal tissues of mice. We analyzed expression of lymphotoxin (LT)α by Th17 cells and lymphoid tissue inducer–like cells. **RESULTS:** $LT\alpha^{-/-}$ and $ROR\gamma t^{-/-}$ mice had significantly lower percentages of naturally occurring Th17 cells in the small intestine than wild-type mice. Numbers of $CD3^{-}CD4^{+/-}$interleukin-$7R\alpha^{+}$c-$kit^{+}CCR6^{+}NKp46^{-}$ lymphoid tissue inducer–like cells that produce interleukin-17A were increased in $LT\alpha^{-/-}$ and $LT\alpha^{-/-}\times$recombination activating gene $(RAG)-2^{-/-}$ mice, compared with wild-type mice, but were absent from $ROR\gamma t^{-/-}$ mice. Parabiosis of wild-type and $LT\alpha^{-/-}$ mice and bone marrow transplant experiments revealed that LTα-dependent gut-associated lymphoid tissue structures are required for generation of naturally occurring Th17 cells. However, when wild-type or $LT\alpha^{-/-}$ $CD4^{+}CD45RB^{high}$ T cells were transferred to $RAG\text{-}2^{-/-}$ or $LT\alpha^{-/-}\times RAG\text{-}2^{-/-}$ mice, all groups, irrespective of the presence or absence of LTα on the donor or recipient cells, developed colitis and generated Th1, Th17, and Th17/Th1 cells. $RAG\text{-}2^{-/-}$ mice that received a second round of transplantation, with colitogenic but not naturally occurring Th17 cells, developed intestinal inflammation. The presence of naturally occurring Th17 cells in the colons of mice inhibited development of colitis after transfer of $CD4^{+}CD45RB^{high}$ T cells and increased the numbers of $Foxp3^{+}$ cells derived from $CD4^{+}CD45RB^{high}$ T cells. **CONCLUSIONS: Gut-associated lymphoid tissue structures are required to generate naturally occurring Th17 cells that have regulatory activities in normal intestines of mice, but not for colitogenic Th17 and Th17/Th1 cells during inflammation.**

Keywords: Immune Regulation; T-Cell Development; Mouse Model; Inflammatory Bowel Disease.

Naturally occurring T helper (Th) 17 cells compose a considerable proportion of lamina propria (LP) $CD4^{+}$ T cells in the small intestine (SI) of healthy mice.[1–3] Retinoid-related orphan receptor (ROR) γt is a key transcription factor for the differentiation program of Th17 cells.[1] Although Th17 cells are absent in $ROR\gamma t^{-/-}$ mice that lack gut-associated lymphoid tissues (GALT), such as Peyer's patches (PP) and cryptopatches,[1] $ROR\gamma t^{-/-}$ mice lack lymphoid tissue inducer (LTi) cells,[4] which are essential for the formation of GALT during ontogeny.[5] $ROR\gamma t^{+}$ lineage $(Lin)^{-}CD4^{+/-}$interleukin (IL)-$7R\alpha^{+}$ LTi-like cells with a similar phenotype to that of embryonic LTi cells were identified in the adult intestine.[6] In addition to the lymphoid organogenesis, another aspect of LTi-like cells in mucosal immune function has attracted attention. LTi-like cells are a subset of innate lymphoid cells (ILCs)[7] and are also an innate source of IL-22, IL-17A, and interferon (IFN)-γ. Of note, $Thy1^{high}Sca\text{-}1^{+}$ IFN-γ–producing LTi-like cells seem to be involved in the induction of innate colitis induced by *Helicobacter hepaticus* infection and the administration of anti-CD40 monoclonal antibody to recombination activating gene (RAG)-$2^{-/-}$ mice.[8,9] Furthermore, a subset of IL-22–producing ILC co-expressing RORγt and natural killer cell receptors has been described as NK22 (natural killer cell receptors–LTi, NCR-22, natural killer cell receptors^{+}$ROR\gamma t^{+}$ ILC, and ILC22) cells.[10]

However, the direct relationship between RORγt-expressing Th17/LTi-like cells and the existence of GALT has not been investigated. Based on previous studies, we used $LT\alpha^{-/-}$ mice, which lack GALT but retain the RORγt function,[11] to investigate the relationship between LTi-like cells and Th17 cells in steady and inflammatory conditions.

Abbreviations used in this paper: BM, bone marrow; GALT, gut-associated lymphoid tissue; GFP, green fluorescent protein; GITR, glucocorticoid-induced tumour necrosis factor receptor; IFN, interferon; IL, interleukin; ILC, innate lymphoid cells; LP, lamina propria; LTα, lymphotoxin α; LTβR, lymphotoxin β receptor; LTi, lymphoid tissue inducer; PP, Peyer's patches; RAG, recombination activating gene; RORγt, retinoid-related orphan receptor gamma t; Rorc, RAR-related orphan receptor C; SI, small intestine; TCR, T-cell receptor; TGF, transforming growth factor; Th, T helper; WT, wild type.

0016-5085/$36.00
http://dx.doi.org/10.1053/j.gastro.2012.07.108

Materials and Methods

See the Supplementary Materials and Methods section for full details.

Animals

C57BL/6J-Ly5.2 mice were obtained from CLEA Japan, Inc (Tokyo, Japan). C57BL/6-Ly5.1 mice and C57BL/6-Ly5.2-RAG-2$^{-/-}$ mice were obtained from Taconic Laboratory (Hudson, NY) and Central Laboratories for Experimental Animals (Kawasaki, Japan). Ly5.2-background lymphotoxin α-deficient (LTα$^{-/-}$) mice were purchased from Jackson Laboratories (Bar Harbor, ME). Mice with a green fluorescent protein (GFP) reporter complementary DNA knocked-in at the site for initiation of RORγt translation on the C57BL/6 background (RAR-related orphan receptor C [*Rorc*]$(\gamma t)^{gfp/+}$ reporter mice, and *Rorc*$(\gamma t)^{gfp/gfp}$ mice [hereafter called RORγt$^{-/-}$ mice]) were kindly provided by Dr Littman.[11] LTα$^{-/-}$ mice were intercrossed into RAG-2$^{-/-}$ mice to generate LTα$^{-/-}$×RAG-2$^{-/-}$ mice. Mice were maintained after Caesarean surgery under specific pathogen-free conditions in our Animal Care Facility. All experiments were approved by the regional animal study committees.

Statistical Analysis

The results are expressed as mean ± standard error of the mean. Groups of data were compared by the Student *t* test. *P* values less than .05 were considered statistically significant.

Results

LTα$^{-/-}$ Mice Lack Naturally Occurring Th17 Cells but Retain CD3$^-$ IL-17A–Expressing Cells in the SI

We first assessed the generation of naturally occurring Th17 cells in the SI of wild-type (WT), RORγt$^{-/-}$, and LTα$^{-/-}$ mice at 18–23 weeks of age. We used fully matured mice because the emergence of intestinal naturally occurring Th17 cells is dependent on the presence of commensal microbiota, and the ratio of those cells increases over time after birth.[2] Naturally occurring IL-17A$^+$IFN-γ$^-$ Th17 cells constitute a considerable proportion in the CD3$^+$CD4$^+$-gated population as well as IL-17A$^-$IFN-γ$^+$ Th1 cells in the LP of SI in WT mice (Figure 1*A*). RORγt$^{-/-}$ mice mostly lacked Th17 cells, but retained a normal proportion of Th1 cells (Figure 1*A*). LTα$^{-/-}$ mice also lacked Th17 cells with a normal proportion of Th1 cells (Figure 1*A*). Although the total LP CD4$^+$ T-cell numbers of all 3 groups were comparable (Figure 1*Bi*), the proportion of Th17 cells of RORγt$^{-/-}$ and LT α$^{-/-}$ mice was reduced significantly compared with that of WT mice (Figure 1*Bii*), whereas that of Th1 cells in all the groups was comparable (Figure 1*Biii*). Consistently, the proportion of IL-17A$^-$IFN-γ$^-$ CD4$^+$ T cells from RORγt$^{-/-}$ and LT α$^{-/-}$ mice was increased significantly (Figure 1*Biv*). It was notable that IL-17A$^+$IFN-γ$^+$ Th17/Th1 cells were not detected in all mice in the steady-state condition (Figure 1*A*).

These results suggest that the LTα-dependent pathway may be required for the generation of naturally occurring Th17 cells. However, when looking at the CD3/IL-17A fluorescence-activated cell sorter profile in the lymphocyte-gated population, we noticed that a substantial pro-

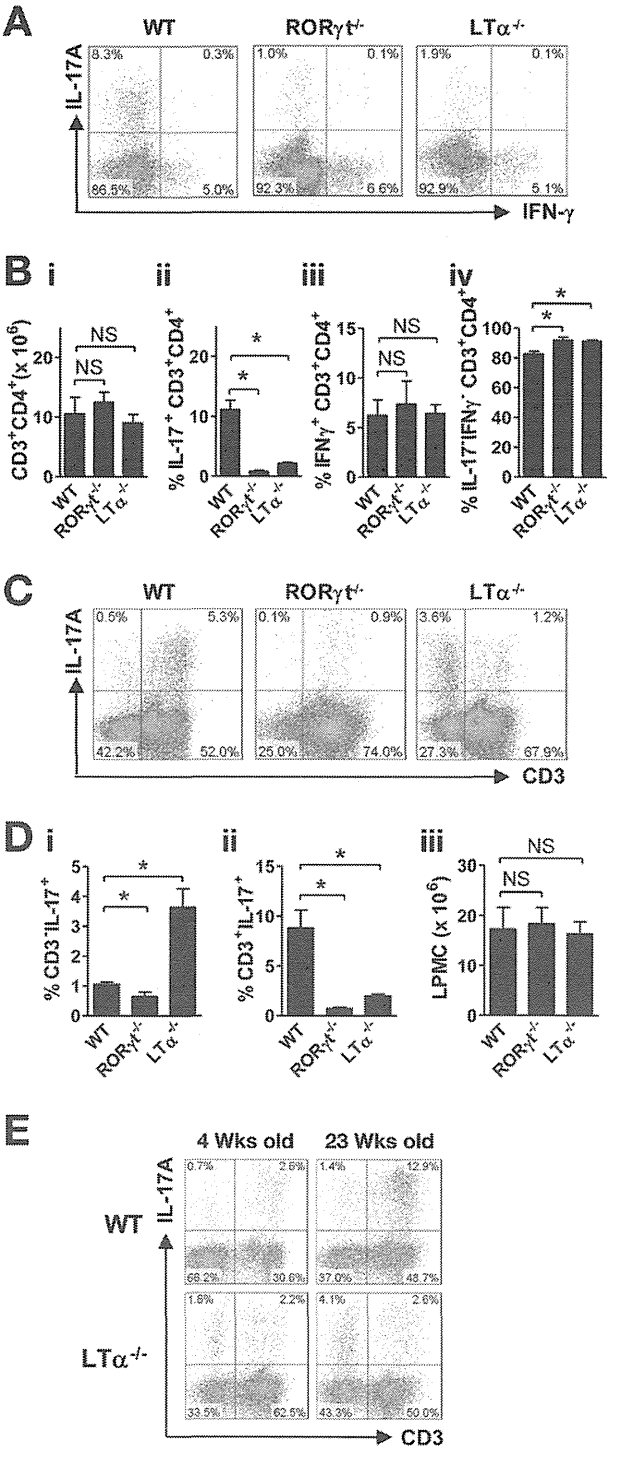

Figure 1. LTα$^{-/-}$ mice lack naturally occurring Th17 cells but retain CD3$^-$ IL-17A–expressing cells in the SI. (*A*) Expression of IL-17A and IFN-γ in SI LP CD3$^+$CD4$^+$ T cells of the indicated mice. (*B*) Absolute cell number of CD3$^+$CD4$^+$ T cells (*i*). Mean percentages of IL-17A$^+$ (*ii*), IFN-γ$^+$ (*iii*), or IL-17A$^-$IFN-γ$^-$ (*iv*) cells in CD3$^+$CD4$^+$ T cells. (*C*) Expression of IL-17A and CD3 in LP mononuclear cells of the indicated mice. (*D*) Mean percentages of IL-17A$^+$CD3$^-$ (*i*) or IL-17A$^+$CD3$^+$ (*ii*) cells in SI LP mononuclear cells. Absolute cell number of LP mononuclear cells of the indicated mice (*iii*). (*E*) Expression of IL-17A and CD3 in LP mononuclear cells of the indicated mice at 4 or 23 weeks old. (*B* and *D*) Data show mean ± standard error of the mean (n = 8/group). *$P < .05$.

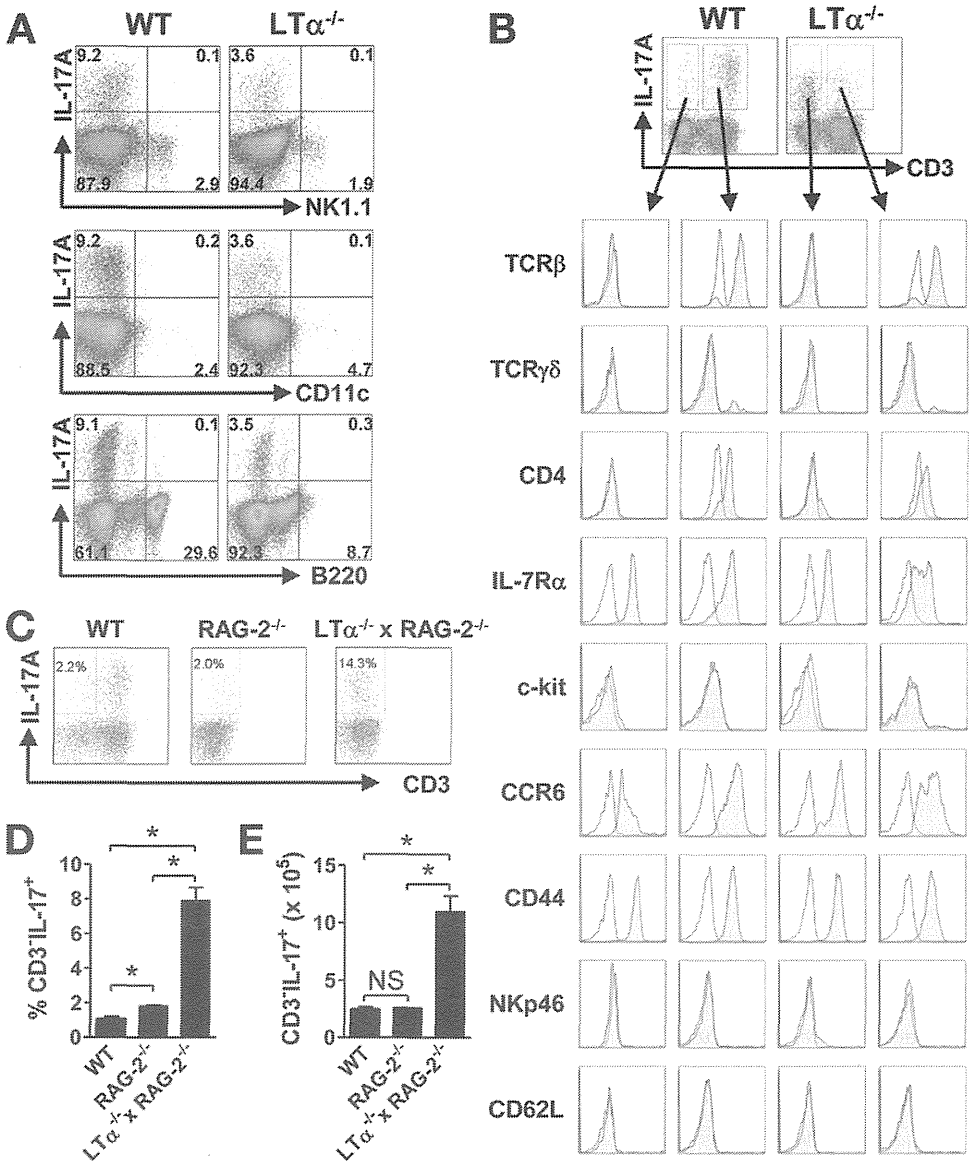

Figure 2. IL-17–expressing CD3$^-$ cells in the SI of LT$\alpha^{-/-}$ mice are LTi-like cells. (*A*) IL-17–producing cells in LT $\alpha^{-/-}$ mice are neither T, natural killer, dendritic, nor B cells. Expression of IL-17A and NK1.1, CD11c, or B220 on LP mononuclear cells from the indicated mice. Data are representative of 6 mice in each group. (*B*) Flow cytometry analysis of LP mononuclear cells from WT or LT$\alpha^{-/-}$ mice. Cells were stimulated in vitro with phorbol myristate acetate/ionomycin and subjected to intracellular cellular staining for IL-17A co-stained with CD3 and NK1.1, CD11c, B220, CD4, IL-7Rα, c-kit, CCR6, CD44, NKp46, CD62L, TCRβ, TCRγδ (*gray histograms*), or isotype control antibodies (*open histograms*). Data are representative of 6 mice in each group. (*C*) Expression of IL-17A and CD3 in LP mononuclear cells of the indicated mice. (*D*) Mean percentages of CD3$^-$IL-17A$^+$ cells in LP mononuclear cells. (*E*) Absolute cell number of CD3$^-$IL-17A$^+$ cells in SI. (*D* and *E*) Data show mean ± standard error of the mean (n = 3/group). *$P <$ .05.

portion of IL-17–expressing cells in LT$\alpha^{-/-}$ mice resided in the CD3-negative subpopulation, whereas IL-17–expressing cells in WT mice resided in the CD3-positive subpopulation (Figure 1*C*). RORγt$^{-/-}$ mice mostly lack both IL-17–expressing subpopulations (Figure 1*C*). This was confirmed by statistical analysis (Figure 1*Di* and *ii*). Furthermore, the absolute cell numbers of LP mononuclear cells were comparable among all 3 groups (Figure 1*Diii*). Intriguingly, the ratio of IL-17–expressing CD3$^-$ cells in LT$\alpha^{-/-}$ mice was increased with age in parallel with that of IL-17–expressing CD3$^+$ Th17 cells in WT mice (Figure 1*E*).

In the spleen, the proportion of CD3$^-$ and CD3$^+$ subpopulations of IL-17–expressing cells was very small, but comparable between WT and LT$\alpha^{-/-}$ mice. In the colon, the proportion of CD3$^+$IL-17$^+$ Th17 cells in LT$\alpha^{-/-}$ mice was reduced significantly compared with that in WT mice, whereas the proportion of CD3$^-$IL-17$^+$ cells was comparable between WT and LT$\alpha^{-/-}$ mice (Supplementary Figure 1).

To exclude the possible contribution of distinct pathogen colonization in WT and LT$\alpha^{-/-}$ mice to the balance of IL-17–expressing CD3$^-$ and CD3$^+$ subpopulations, we prepared 20-week-old WT and LT$\alpha^{-/-}$ mice co-housed for 16 weeks in the same cages. The findings were the same as observed in Figure 1 (Supplementary Figure 2).

IL-17–Expressing CD3$^-$ Cells in LT$\alpha^{-/-}$ Mice Are LTi-Like Cells

To delineate the population of IL-17–expressing CD3$^-$ cells in LT$\alpha^{-/-}$ mice, we assessed the expression of lineage markers. First, IL-17–expressing cells in the SI of LT$\alpha^{-/-}$ or WT mice did not express NK1.1, CD11c, or B220 (Figure 2*A*). Furthermore, most IL-17A$^+$CD3$^+$ cells in LT$\alpha^{-/-}$ or WT mice expressed T-cell receptor (TCR)β, but a small proportion of those cells expressed TCR$\gamma\delta$, whereas most IL-17A$^+$CD3$^-$ cells in LT$\alpha^{-/-}$ or WT mice did not express TCRβ (Figure 2*B*). Also, most IL-

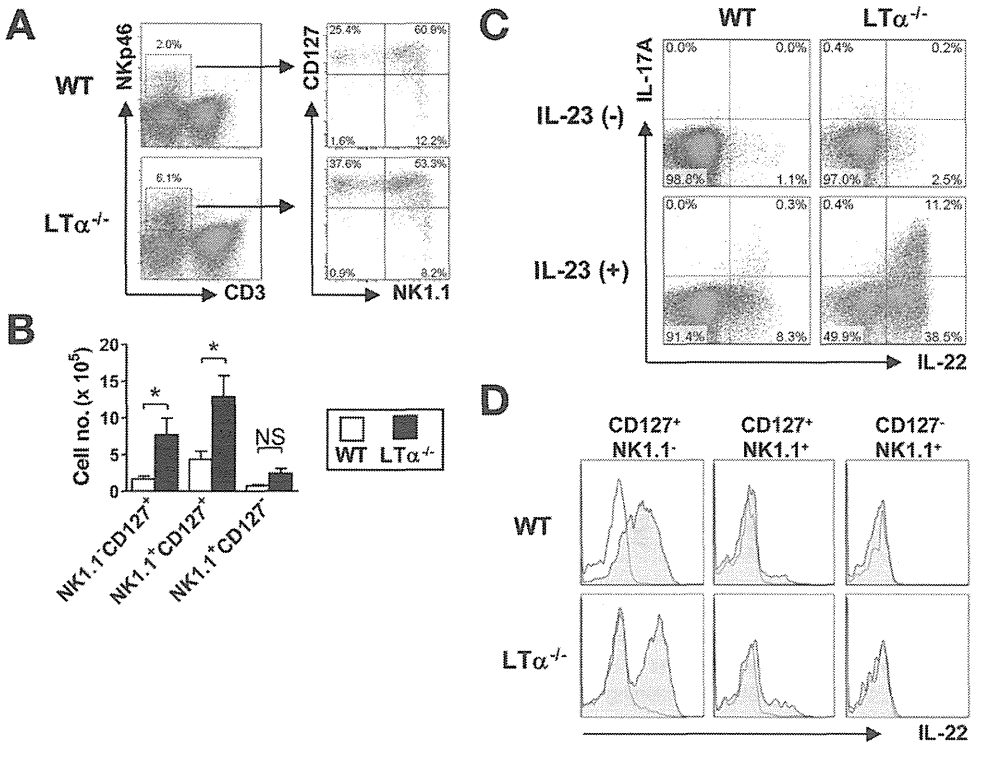

Figure 3. Numbers of intestinal NKp46$^+$ NK22 cells increase in the SI of LT$\alpha^{-/-}$ mice. (*A*) Expression of CD3 and NKp46 cells in SI neither T, natural killer, dendritic, nor B cells of the indicated mice (*left*). Expression of NK1.1 and CD127 gated on CD3$^-$NKp46$^+$ cells (*right*). Data are representative of 6 mice in each group. (*B*) Absolute cell number of CD3$^-$NKp46$^+$CD127$^+$NK1.1$^-$, NK1.1$^+$, and CD3$^-$NKp46$^+$ CD127$^-$NK1.1$^+$ cells. *White bar*, WT mice; *black bar*, LT$\alpha^{-/-}$ mice. Data show mean ± standard error of the mean (n = 4/group). *$P <$ .05. (*C*) Expression of IL-17A and IL-22 in SI LP CD3$^-$ cells of the indicated mice. Cells were cultured in vitro with or without IL-23. (*D*) Expression of IL-22 in SI LP CD3$^-$NKp46$^+$ cells of the indicated population. Cells were cultured in vitro with or without IL-23. *Gray histograms* indicate the subset cultured with IL-23. *Open histograms* indicate the subset cultured without IL-23.

17A$^+$CD3$^+$ cells in LT$\alpha^{-/-}$ or WT mice expressed CD4, CD44, CCR6, and IL-7Rα, but not CD62L, whereas IL-17A$^+$CD3$^-$ cells in LT$\alpha^{-/-}$ or WT mice expressed CD44, CCR6, and IL-7Rα, but most of those cells in WT mice did not express CD4 and only 10% of those cells in LT$\alpha^{-/-}$ mice expressed CD4 (Figure 2*B*). WT or LT$\alpha^{-/-}$ IL-17A$^+$CD3$^-$ cells, but not IL-17A$^+$CD3$^+$ cells, expressed c-kit, whereas only IL-17A$^+$CD3$^-$ subpopulations in LT$\alpha^{-/-}$ mice, but not those cells in WT mice and IL-17A$^+$CD3$^+$ Th17 cells in both mice, retained a small proportion of NKp46 (Figure 2*B*). These results suggest that IL-17A$^+$CD3$^+$ cells are categorized as Th17 cells or IL-17A–producing TCR$\gamma\delta^+$ T cells, whereas IL-17A$^+$CD3$^-$ cells are adult LTi-like cells.

Because it still was possible that the increased IL-17A$^+$CD3$^-$ cells in LT$\alpha^{-/-}$ mice are T lymphocytes that have down-modulated the expression of CD3 and TCRβ, we assessed if IL-17A$^+$CD3$^-$ cells reside in the SI of RAG-2$^{-/-}$ and LT$\alpha^{-/-}$×RAG-2$^{-/-}$ mice in the absence of T cells. Although IL-17A$^+$CD3$^+$ Th17 cells disappeared in both LT$\alpha^{-/-}$×RAG-2$^{-/-}$ and RAG-2$^{-/-}$ mice, IL-17A$^+$CD3$^-$ cells were retained in the SI of both mice (Figure 2*C*), and the proportion (Figure 2*D*) and absolute number of those cells (Figure 2*E*) in LT$\alpha^{-/-}$×RAG-2$^{-/-}$ mice were increased significantly compared with those in RAG-2$^{-/-}$ mice. This suggested that the increased numbers of IL-17A$^+$CD3$^-$ cells in LT$\alpha^{-/-}$×RAG-2$^{-/-}$ mice were LTi-like cells, and were independent of the presence of Th17 cells.

Intestinal NK22 Cells Also Increase in LT$\alpha^{-/-}$ Mice

Recently, NK22 cells co-expressing RORγt have gained attention,[10] although controversially recent articles reported that NK22 cells are the progeny of LTi-like cells,[12] although other articles have disagreed.[13] Intriguingly, both CD3$^-$NKp46$^+$IL-7Rα^+NK1.1$^-$ and NK1.1$^+$ subsets in the SI of LT$\alpha^{-/-}$ mice were increased significantly compared with those in WT mice (Figure 3*A* and *B*). Furthermore, in vitro stimulation by IL-23 strongly induced IL-22$^+$IL-17A$^-$ cells and IL-22$^+$IL-17A$^+$ cells in the CD3-negative population from WT and LT$\alpha^{-/-}$ mice (Figure 3*C*). Furthermore, IL-22–expressing CD3$^-$NKp46$^+$ cells were CD127$^+$NK1.1$^-$ irrespective of whether they were isolated from WT or LT$\alpha^{-/-}$ mice (Figure 3*D*). This suggested the following: (1) the CD3$^-$ population contained IL-23R–expressing cells; (2) the increase of IL-23–responding LTi-like cells in the SI of LT$\alpha^{-/-}$ mice resulted in the development of NK22 cells; and (3) LTα expression on LTi-like cells was dispensable for the differentiation of NK22 cells.

LTα Molecules on CD4$^+$ T Cells Are Not Required for the Development of Naturally Occurring Th17 Cells

We further investigated whether LTα molecules on CD4$^+$ T cells and LTi-like cells are required for the development of naturally occurring Th17 cells. To this end, we used a parabiosis system that joined Ly5.1$^+$ WT and Ly5.2$^+$ LT$\alpha^{-/-}$ mice (Figure 4*A*). Four weeks after parabiosis surgery, SI Th17 cells in LT$\alpha^{-/-}$ mice in the parabionts were significantly restored as compared with those in LT$\alpha^{-/-}$ mice without parabiosis (Figure 4*B*), whereas SI Th1 cells were comparable among all mice (Figure 4*C*). Furthermore, a substantial number of Th17 and Th1 cells in both mice emerged on opposite sides of the parabionts (Figure 4*B* and *C*). In contrast, it was notable that the LTi-like cell subset was restricted to the original SI (Figure

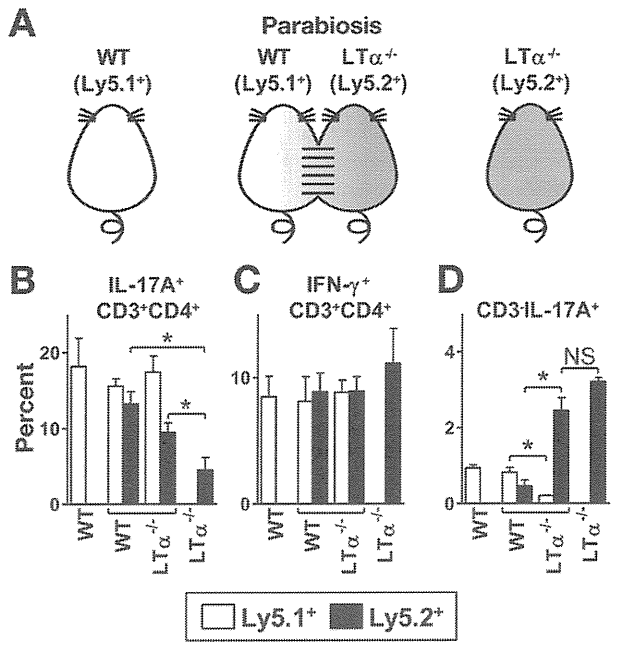

Figure 4. LTα expression on CD4+ T cells is not required for the development of intestinal naturally occurring Th17 cells. (*A*) Scheme of the parabiosis experiment. Ly5.2+ LTα$^{-/-}$ mice were joined with age-matched Ly5.1+ WT mice (n = 7). Age-matched Ly5.1+ WT mice and Ly5.2+ LTα$^{-/-}$ mice without parabiosis surgery were used as controls (n = 4/group). (*B*) Mean percentages of Th17 cells in SI LP CD3+CD4+ cells. (*C*) Mean percentages of Th1 cells in SI LP CD3+CD4+ cells. (*D*) Mean percentages of IL-17A+ cells in SI LP CD3− cells. *White bar*, Ly5.1+ cells; *black bar*, Ly5.2+ cells. (*B–D*) Data show mean ± standard error of the mean (n = 4 or 7/group). *$P < .05$.

4*D*), suggesting that LTi-like cells are resident cells, whereas Th17 cells are well mixed by the blood circulation or that progenitor-naive CD4+ T cells migrate to both SI sites for the generation of Th17 cells. Therefore, these results suggest that naive LTα$^{-/-}$ CD4+ T cells reach the SI of WT mice, and differentiate into Th17 cells at the site where normal LTi-like cells reside. Furthermore, this parabiosis experiment indicates that LTα expression on CD4+ T cells is not required for Th17 cell differentiation.

Given that LTα expression on CD4+ T cells is not required for naturally occurring Th17 cell differentiation, we directly assessed whether the lack of LTα on CD4+ cells impaired the development of in vitro–manipulated Th17 cells. Consistent with the parabiosis experiment, WT and LTα$^{-/-}$-naive CD4+ T cells differentiated into Th17 cells at a comparable level after transforming growth factor (TGF)-β and IL-6 stimulation (Supplementary Figure 3).

The LTα-Dependent GALT Structures Are Required for the Generation of Intestinal Naturally Occurring Th17 Cells

We further investigated whether LTα expression on bone marrow (BM)-derived cells was required for the development of naturally occurring Th17 and LTi-like cells. To this end, irradiated WT or LTα$^{-/-}$ mice were reconstituted with BM from WT or LTα$^{-/-}$ mice to set up 4 experimental groups as depicted in Supplementary Figure 4*A*. Naturally occurring Th17 cells developed in group 3 (LTα$^{-/-}$→WT) and group 1 (WT→WT) in similar numbers, but were not observed in group 2 (WT→LTα$^{-/-}$) or group 4 (LTα$^{-/-}$→LTα$^{-/-}$) (Supplementary Figure 4*B* and *C*). In groups 2 and 4 (LTα$^{-/-}$ recipients), IL-17A+CD3− subpopulations were increased compared with groups 1 and 3 (WT recipients) (Supplementary Figure 4*D* and *E*).

To further confirm this observation, freshly isolated Lin−CD45+NKp46− GFP (RORγt)^{high} LTi-like cells from the SI of *Rorc(γt)*$^{gfp/+}$ mice were transferred into LTα$^{-/-}$ mice (Supplementary Figure 5*A*). Consistent with the BM chimera experiment, the proportion of naturally occurring Th17 cells in the SI of LTα$^{-/-}$ mice with LTi-like cell transfer and LTα$^{-/-}$ mice without transfer was comparable and significantly lower than that in the SI of WT mice (Supplementary Figure 5*B* and *C*). Collectively, LTα-expressing BM-derived cells including LTi-like cells were not essential for the development of naturally occurring Th17 cells, but rather the GALT structure is essential as the induction site of naturally occurring Th17 cells.

LTα Molecules on LTi-Like and CD4+ T Cells Are Not Required for the Development of Colitogenic Th17 and Th17/Th1 Cells

We next investigated if this is a case with colitogenic Th17 cells developed under colitic conditions. To this end, we created 4 groups in an adoptive transfer colitis model as depicted in Figure 5*A*. Six weeks after transfer, all groups of mice developed colitis (Figure 5*B*) as confirmed by histologic scores (Figure 5*C*), although LTα$^{-/-}$×RAG-2$^{-/-}$ recipients transferred with WT or LTα$^{-/-}$ donor CD4+CD45RB^{high} T cells (group 2 or 4 mice) had significantly milder colitis than the paired RAG-2$^{-/-}$ recipients (group 1 or 3 mice) (Figure 5*C*). The clinical scores of mice confirmed that all groups of mice developed colitis, but the lack of LTα on CD4+CD45RB^{high} T cells did not affect the clinical scores, which were consistent between groups 1 and 3 RAG-2$^{-/-}$ and between groups 2 and 4 LTα$^{-/-}$×RAG-2$^{-/-}$ mice, respectively (Figure 5*B*). Consistently, the absolute cell numbers of colonic LP CD3+CD4+ from all 4 groups were significantly higher than in control WT mice, but colonic LP CD3+CD4+ cells from all groups 2 and 4 mice were significantly lower than in groups 1 and 3 mice, respectively.

In sharp contrast to the finding that there is a lack of naturally occurring Th17 cells in the SI LP of LTα$^{-/-}$ mice in the steady state (Figure 1*A*), surprisingly, not only a comparable proportion of Th17 cells emerged in colitic LP of all 4 groups, but also a comparable proportion of IL-17A+IFN-γ+ Th17/Th1 cells (Figure 5*Fi* and *ii*). Likewise, the proportion of colitic IL-17A−IFN-γ+ Th1 cells was comparable among all 4 groups (Figure 5*Fi* and *ii*). These results indicate that not only the existence of GALT but also LTα expression on CD4+ and LTi-like cells are not essential for the development of colitogenic LP Th17 and Th17/Th1 cells, unlike in the steady conditions.